Available online at www.sciencedirect.com
ScienceDirect
Materials Chemistry and Physics 110 (2008) 106–109
MATERIALS CHEMISTRY AND PHYSICS
www.elsevier.com/locate/matchemphys

Synthesis and characterization of nanocrystalline NiSb and $NiSb_2$ at low temperature

Chunhui Li [a,b], Jin Hu [c], Qing Peng [a,*], Xun Wang [a]

[a] *Department of Chemistry, Tsinghua University, Beijing 100084, PR China*
[b] *College of Materials Engineering, Zhengzhou University, Zhengzhou 450001, PR China*
[c] *Beijing National Laboratory for Condensed Matter Physics, Institute of Physics, Chinese Academy of Sciences, Beijing 100080, China*

Received 27 August 2007; received in revised form 3 January 2008; accepted 18 January 2008

Abstract

Nanocrystalline NiSb and $NiSb_2$ have been prepared through a solvothermal co-reduction route at low temperatures (120–180 °C). The features of this method include: (1) the reactants are simple inorganic salts ($NiCl_2{\cdot}6H_2O$ and $SbCl_3$); (2) two types of nickel antimonides (NiSb and $NiSb_2$) can be obtained respectively by changing the reducing agents and temperatures. The as-prepared samples were characterized by XRD and TEM. A possible formation mechanism has been presented. The thermoelectric properties of as-prepared NiSb, and the magnetic properties of $NiSb_2$ were investigated.

Keywords: Binary antimonide; Solvothermal; Co-reduction; Characterization

1. Introduction

Metal pnictides, which are well-known electric and optoelectronic materials [1], have important applications, such as in compact displayers, satellite TV receivers, and optical fiber communications [2]. In comparison with traditional III–V semiconductors, transition metal pnictides have many special electrical, mechanical, and anticorrodating properties [3]. Among them, nickel antimonides have gained much more attention because of their technological importance in secondary high-temperature batteries [4].

Conventionally, transition metal pnictides are prepared by direct reaction of melted elements in an evacuated quartz tube, and then quenched at high temperature (usually above 1000 °C) for several days. Considerable efforts have been made to decrease the reaction temperature and reduce the reaction time. Several new methods, such as dehalosilylation related reactions, solution–liquid–solid mechanism, and metal organic precursors' alcoholysis, have been developed [5–7]. However, due to the formation difficulty of SbH_3 and metal organic antimony precursors, these methods cannot be used to prepare binary metal antimonides.

Recently, Kaner and co-workers obtained GaSb and InSb at 550 °C by using a solid-state metathesis (SSM) way. In their final products, elemental Sb still co-exists [8], which confirms that metal antimonides are not easy to form due to the strong metallicity of antimony. Gopalakrishnan et al. prepared $NiSb_2$ by directly reducing the antimonite precursors using H_2 at 500 °C [9]. To date, how to synthesize pure-phase binary metal antimonides more controllable at low temperature is still a challenge to material scientists [10]. In this paper, we report a mild solvothermal co-reduction reaction route to selectively synthesize single-phase nanocrystalline NiSb and $NiSb_2$. Different reductants (Zn or $NaBH_4$) were chosen in the reaction and were found to be a key factor to the final composition of the product. This method will have a good prospect and surely can be used to synthesize other nanocrystalline metal antimonides.

2. Experimental section

2.1. Synthesis

In a typical reaction, 4 mmol $NiCl_2{\cdot}6H_2O$ and 4 mmol $SbCl_3$ were mixed in 40 ml ethanol, and then excess reducing agent (Zn,

* Corresponding author. Tel.: +86 10 62792798; fax: +86 10 62788765.
E-mail address: pengqing@mail.tsinghua.edu.cn (Q. Peng).

0254-0584/$ – see front matter © 2008 Elsevier B.V. All rights reserved.
doi:10.1016/j.matchemphys.2008.01.022

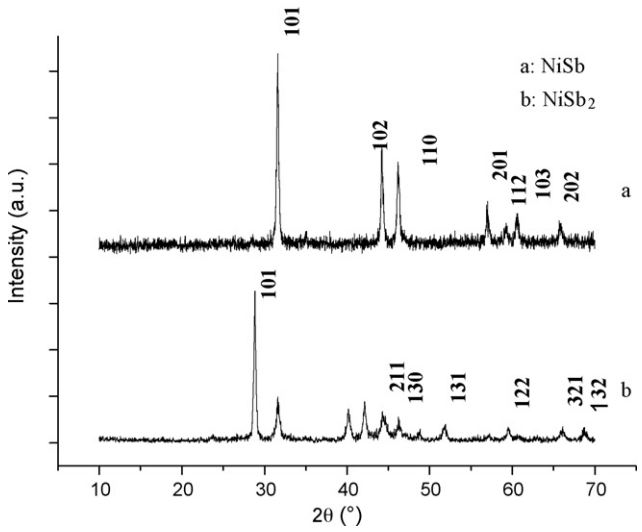

Fig. 1. XRD patterns of NiSb and $NiSb_2$.

Mg or $NaBH_4$) was added. After stirring for several minutes, the mixture was then transferred into a 50-ml autoclave and filled up to 80% of the total volume. The autoclave was sealed and heated at a certain temperature for about 48 h. (Caution! $SbCl_3$ should be handled very carefully for its corrosiveness.) The system was then allowed to cool to room temperature. The final product was collected by filtration, and washed with diluted HCl solution and deionized water to remove any possible ionic remnants, and finally dried at 50 °C.

2.2. Characterization

Power X-ray diffraction (XRD) was performed on a Bruker D8-Advance X-ray powder diffractometer with Cu Kα radiation (λ = 1.5418 Å). The 2θ range used in the measurement of NiSb and $NiSb_2$ was from 10° to 70° in steps of 0.02°. TEM images were taken with a Hitachi model H-800 transmission electron microscope using an accelerating voltage of 200 kV.

3. Results and discussion

During the reaction process, the composition (NiSb or $NiSb_2$) of the final product can be easily controlled by using different reducing agents under different reaction temperatures. From the XRD patterns (Fig. 1), all the reflections of the products can be readily indexed to pure-phase of NiSb and $NiSb_2$, with lattice constants $a = 3.925$, $c = 5.137$ Å (JCPDS no. 41-1439, NiSb) and $a = 5.180$, $b = 6.314$ and $c = 3.838$ Å (JCPDS no. 04-0687, $NiSb_2$). The XRD patterns indicate that pure NiSb and $NiSb_2$ can be obtained under the current synthetic conditions. TEM images for the samples are shown in Fig. 2. The products are all well-dispersed nanoparticles with diameters of approximately 60–80 nm. As shown in Fig. 2, some nanocrystals have comparatively regular shape, indicating samples have relatively higher crystallization.

Table 1
Experimental results using different reducing agents and temperatures[a]

	$NaBH_4$	Mg	Zn
110 °C	NiSb	$NiSb_2$	$NiSb_2$
140 °C	NiSb	NiSb	$NiSb_2$
180 °C	NiSb	NiSb	NiSb

[a] The reaction times are all 48 h.

Considering the fact that NiSb and $NiSb_2$ nanocrystals were obtained via similar co-reduction reactions using the same start materials but different reductants, a series of controllable reactions have been performed under different temperatures to investigate the effect of reductants on the composition of the products. The results are shown in Table 1.

As shown in Table 1, only NiSb could be obtained when $NaBH_4$ was used as the reductant under all reaction temperatures. When Zn or Mg powder was used as the reductant in our experiments, NiSb was obtained at higher temperature and $NiSb_2$ was obtained at lower temperature. This phenomenon indicates that the formation of NiSb is greatly facilitated under higher temperatures in higher reducibility environment, which can be attributed to the fact that NiSb is the thermodynamically favored phase compared to $NiSb_2$. The possible reaction process may be described as the following equations (take Zn as the example):

$$Zn + 2CH_3CH_2OH \rightleftharpoons Zn(OCH_2CH_3)_2 + 2H \quad (1)$$

$$NiCl_2 + 2SbCl_3 + 8H \rightarrow NiSb_2 + 8HCl \quad (2)$$

$$Zn(OCH_2CH_3)_2 + 2HCl \rightarrow ZnCl_2 + 2CH_3CH_2OH \quad (3)$$

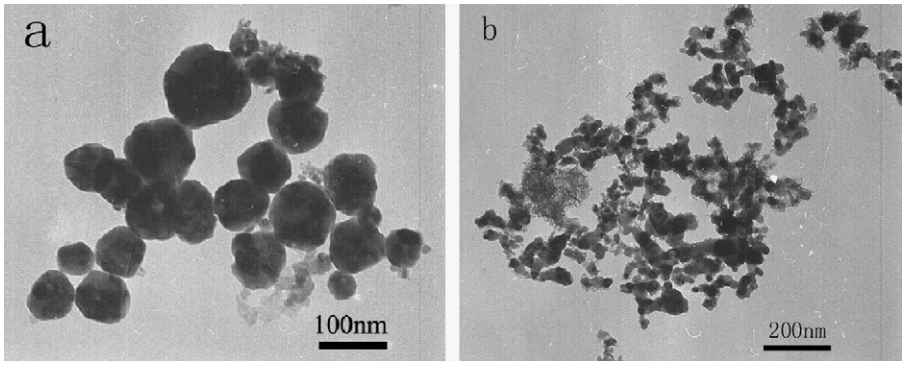

Fig. 2. TEM images of (a) NiSb and (b) $NiSb_2$ nanoparticles.

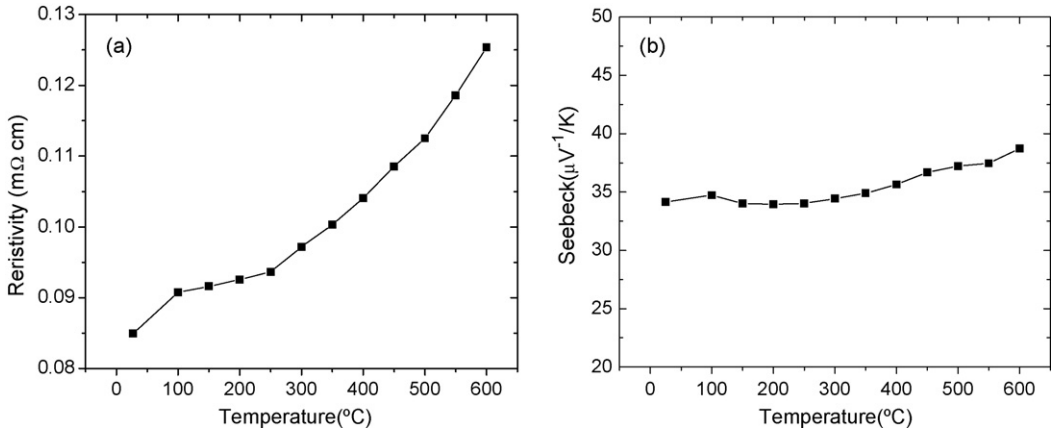

Fig. 3. (a) Resistance–temperature curve and (b) Seebeck coefficient of NiSb.

the overall reaction can be expressed as

$$NiCl_2 + 2SbCl_3 + 4Zn \rightarrow NiSb_2 + 4ZnCl_2 \quad (4)$$

The above reaction steps can be confirmed by the following experiments. When $CHCl_3$ or benzene was used instead of ethanol, no phase of NiSb could be obtained. This indicates that ethanol not only acts as a reaction medium but also reacts with Zn to produce active hydrogen in our reaction system. There are other two reasons to choose ethanol as the reaction medium in our reaction. First, the critical temperature of ethanol (243 °C) is much lower than that of water (374 °C), and the diffusion rates of ions in ethanol under 110–180 °C are more rapid than that in water due to its lower viscosity. This will be beneficial to the solubilization of the starting materials and subsequently the crystal growth process. Secondly, the hydrolysis reaction of $SbCl_3$ restricted the use of water as a reaction medium and ethanol does not meet the problem.

To the best of knowledge, the thermoelectric properties of NiSb which may reveal improved and tailored properties for a number of applications have not been investigated before. For these, the electric and magnetic properties of nickel antimonides have been measured in our experiments. In our experiments, the nano-powders are cold pressed into pellet under 4 MPa pressure. Fig. 3 shows the resistance–temperature curve and Seebeck coefficient of as-prepared NiSb nanocrystals. As shown in Fig. 3a, the resistance of material increases with the rise of temperature, which exhibits the characteristic behavior of metal. This indicates that NiSb can be understood as an alloy. Fig. 3b shows the Seebeck coefficient curve of NiSb nanocrystals. The Seebeck coefficient of NiSb is relatively small and does not vary greatly with the change of temperature.

Transition metal pnictides can exhibit interesting magnetic properties [11]. Fig. 4 shows the hysteresis curve of as-prepared $NiSb_2$ in the range of −10,000 to 10,000 G. Magnetic studies show that the saturated magnetization of as-prepared $NiSb_2$ nanocrystals is 2.47 emu g^{-1}, exhibiting possible weak ferromagnetic coupling. The remanence and coercive field of $NiSb_2$ sample are 0.724 emu g^{-1} and 222.9 G, respectively.

Pure bulk $NiSb_2$ is diamagnetic due to its $3d^6$ low-spin electron configuration, whereas our experimental data show that $NiSb_2$ nanocrystals are ferromagnetic. It is reasonable to image whether the magnetization comes from ferromagnetic impurities. However, our experimental results show that this is not the case. As-prepared $NiSb_2$ nanocrystals prepared using Zn and Mg powder as different reductants all show obvious magnetic properties and each samples could be allured by a magnet completely.

Based on our experimental facts, it is tentatively believed that the origin of the magnetization may be relevant to small size effect and surface effect of nanomaterials. There are lots of unsaturated bonds on the nano-sized $NiSb_2$ particles surface and the field strength of Ni^{2+} ions surrounding "coordination fields" are not invariable, which differed greatly from bulk $NiSb_2$. Compared with bulk $NiSb_2$, the splitting of e_g and t_{2g} orbitals of Ni^{2+} are more serious, the energy gap between e_g and t_{2g} orbitals becomes less, which is in favor of the electron transition from t_{2g} orbitals to e_g orbitals, thus the classical low-spin electron configuration was changed to some extent and unpaired electrons generated. Detailed mechanism studies are underway.

Lithium-ion batteries are now the prevailing power source in the portable electronic devices such as mobile phones, notebook computers, and camcorders. Considering the high theoretical

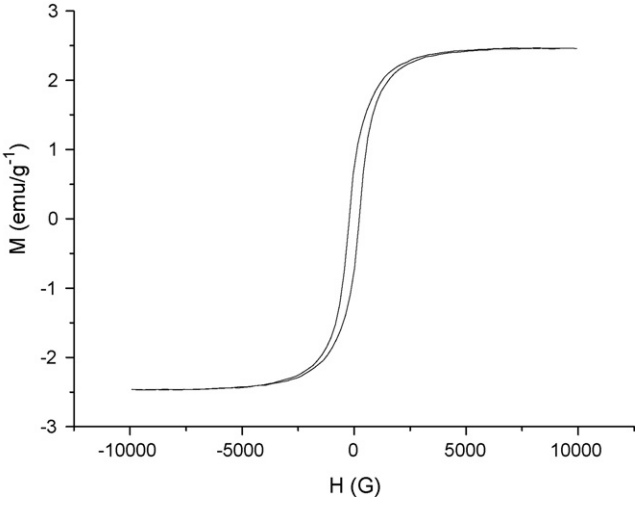

Fig. 4. The hysteresis curve of as-prepared nanocrystalline $NiSb_2$.

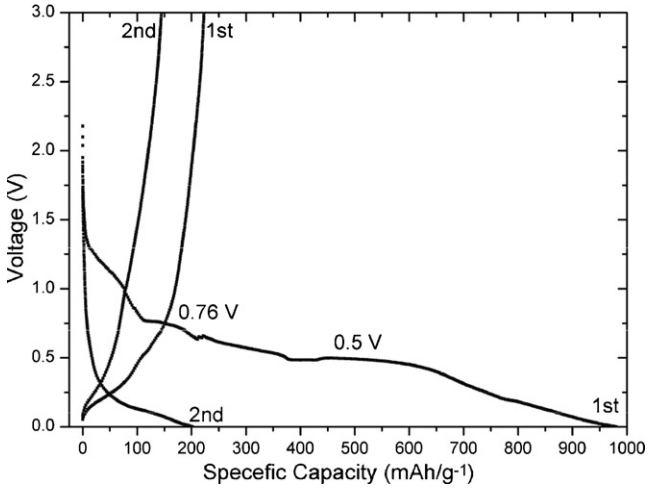

Fig. 5. Charge/discharge curve for $NiSb_2$ electrode for the first two cycles.

capacity of metallic Sb, some Sb-based intermetallic compounds are intensively investigated as potential anode materials for lithium-ion batteries recently. In the paper, as-prepared $NiSb_2$ nanocrystals were investigated as an alternative anode material for lithium-ion batteries.

The electrochemical reactions of $NiSb_2$ with lithium were investigated using a Li/$LiPF_6$ (EC + DMC)/$NiSb_2$ model cell. The working electrode was made by the deposition of a slurry, consisting of 85 wt% $NiSb_2$ power, 5 wt% acetylene black as conducting agent and 10 wt% PVDF (polyvinylidene fluoride) as binder, onto a porous copper substrate. The electrodes were then vacuum-dried at 110 °C for 12 h. The model cells were assembled in the Ar-filled glove box with 99.9% pure lithium foils as counter electrode. The electrolyte used was 1 M $LiPF_6$ in the mixture of ethylene carbonate and dimethyl carbonate (1:1 in weight). The cells were galvanostatic cycled between 0 and 3.0 V at 25 °C at a current density of 0.2 mA cm^{-2}.

Fig. 5 shows the charge–discharge curves of $NiSb_2$ electrode in the initial cycles. As seen in Fig. 5, the first discharge (Li-insertion) capacity reaches 981 mAh g^{-1}, which is almost twice as its theoretical Li-storage capacity (alloy reaction, 532 mAh g^{-1}). The large Li-storage capacity in the first discharge processes can be attributed to the electrochemical alloy reaction (Li + Sb = LiSb, 3Li + Sb = Li_3Sb), which accompanies large volume change. On the other hand, the extra capacity exceeding the theoretical capacity should originate from the formation of solid electrolyte interface (SEI) layer [11,12].

However, the first charge (Li-extraction) capacity is only 223 mAh g^{-1}. $NiSb_2$ nanocrystals exhibit poor capacity retention during the subsequent cycles. Generally, nanometer materials prepared via solvothermal reaction method at relatively low temperature possess high-density dangling bonds and defects intrinsically. Moreover, the insertion and extraction of Li ions into host lattice destroy the crystal structure of the nanocrystalline irreversibly and produce extrinsic defects. These defects should have high energy. Once Li ions are trapped by them, it is difficult to extract all of them out by normal charge mode. It means this feature cannot be avoided for alloy anodes accompanying large phase transitions [12]. In addition, the Li–Sb electrochemical alloy reaction shows higher irreversibility than other alloy reaction such as Li–Sn. The residue of Li alloy is related to chemical properties of host elements. Si and Sb elements show stronger irreversible trapping ability to Li ions than Sn element according to our studies [13,14].

4. Conclusions

In summary, pure-phased binary antimonide NiSb and $NiSb_2$ were prepared through co-reductive reactions employing different reductants. The formation mechanism of $NiSb_2$ is tentatively proposed and it is proved that the solvents played an important role in this route. XRD and TEM examination showed that the products were well-crystallized with diameters of approximately 60–80 nm. The thermoelectric properties of as-prepared NiSb and the magnetic properties of $NiSb_2$ were investigated. The electrochemical performances of $NiSb_2$ were studied and it exhibits relatively high Li-storage capacity.

Acknowledgements

Thanks to Prof. Yadong Li for his valuable advice. This work was supported by Tsinghua Basic Research Foundation and the State Key Project of Fundamental Research (2006CB932608).

References

[1] B.G. Streetman, Solid State Electronic Devices, 3rd ed., Prentice Hall, Englewood Cliffs, NJ, 1990.
[2] A.C. Jones, Chem. Soc. Rev. (1997) 101;
T.J. Cumberbatch, A. Putuis, Mater. Res. Soc. Symp. Proc. 164 (1990) 129;
E.K. Bryne, L. Parkanyi, K.H. Theopld, Science 241 (1988) 332;
D. Gammon, E.S. Snow, B.V. Shanabrook, D.S. Kater, D. Parks, Science 273 (1996) 87.
[3] J.C. Bailer, H.J. Emelius, R. Nyholm, A.F. Trotman-Dickenson, Comprehensive in Organic Chemistry, vol. 2, Pergamon Press, Oxford, 1973.
[4] J. Coetzer, V.I. Louw, Programme 3 Patent Holdings, PCT Int. Appl. WO94 23, 467 (Cl. H01M10/39) October 13, 1994; ZA Appl. 93/2406, April 02, 1993.
[5] M.A. Olshavsky, A.N. Goldstein, A.P. Alivisatos, J. Am. Chem. Soc. 112 (1990) 9438.
[6] T.J. Trentler, K.M. Hickman, S.C. Goel, A.M. Viano, P.C. Gibbons, W.E. Buhro, Science 270 (1995) 1791;
T.J. Trentler, S.C. Goel, K.M. Hickman, A.M. Viano, M. Chiang, A.M. Beatty, P.C. Gibbons, W.E. Buhro, J. Am. Chem. Soc. 119 (1997) 2172.
[7] E.K. Byrne, T. Dougals, K.H. Theopold, Mater. Res. Soc. Symp. Proc. 131 (1989) 59;
T. Dougals, K.H. Theopold, Inorg. Chem. 30 (1991) 594.
[8] R.E. Treece, G.S. Macala, L. Rao, D. Franke, H. Eckert, R.B. Kaner, Inorg. Chem. 32 (1993) 2745.
[9] J. Gopalakrishnan, S. Pandey, K.K. Rangan, Chem. Mater. 9 (1997) 2113.
[10] K.L. Stamm, J.C. Gamo, G.Y. Liu, S.L. Brock, J. Am. Chem. Soc. 125 (2003) 4038.
[11] J. Xie, X.B. Zhao, G.S. Cao, M.J. Zhao, S.F. Su, J. Alloys Compd. 393 (2005) 283.
[12] H. Li, L. Shi, Q. Wang, L. Chen, X. Huang, Solid State Ionics 148 (2002) 247.
[13] H. Li, X.J. Huang, L.Q. Chen, G.W. Zhou, Z. Zhang, D.P. Yu, Y.J. Mo, Solid State Ionics 181 (2000) 135.
[14] H. Li, L.H. Shi, W. Lu, X.J. Huang, L.Q. Chen, J. Electrochem. Soc. 148 (2001) A915.